

# SEGMENTATION INDEPENDENT ESTIMATES OF TURBULENCE PARAMETERS

G. C. Papanicolaou<sup>a</sup>, K. Solna<sup>b</sup> and D. Washburn<sup>c</sup>

<sup>a</sup>Department of Mathematics, Stanford University, Stanford, CA 94305

<sup>b</sup>Department of Mathematics, University of Utah, Salt Lake City, UT 84112

<sup>c</sup>Phillips Laboratory, Kirtland AFB, NM 87117

## ABSTRACT

We present a new approach for analyzing local power law processes and apply it to temperature measurements from the upper atmosphere. We segment the data and use the wavelet scale spectrum to estimate the parameters of the power law, the scale factor and the exponent. These parameters vary from segment to segment. Part of this variation is due to the non-stationarity of the data. Another part is due to estimation errors that depend on the segmentation. In this paper show how to remove effectively these segmentation dependent variations.

**Keywords:** Turbulence, locally stationary time series, scale spectrum, data segmentation, wavelets

## 1. THE DATA SET

We will analyze temperature data obtained by the Air Force high-altitude laser propagation and turbulence data collection effort. For a detailed discussion of recording procedures and analysis see.<sup>1</sup> Here we take the data as our starting point and examine what analysis reveals about their structure. We are interested in particular in accounting properly for nonstationary effects. In Figure 1 we show the temperature data, which has approximately  $5.6 \times 10^6$

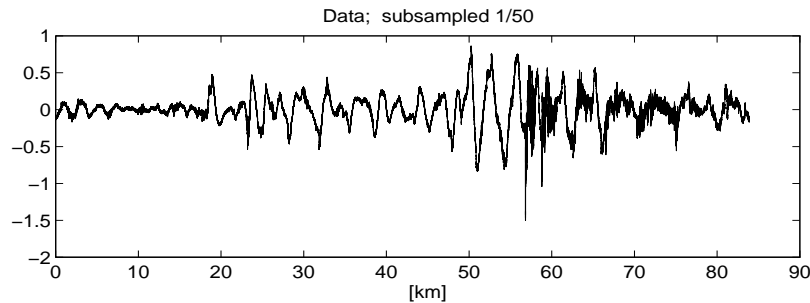


**Figure 1.** Top figure: the raw temperature data over the first 84km out of a 112km record, subsampled 1/50. The spatial resolution of the data is approximately 2cm.

points. The data is, of course, quite noisy and it is part of our task to remove noise effects in the estimation process.

---

G.S.P.: E-mail: [papanico@math.stanford.edu](mailto:papanico@math.stanford.edu)

K.S.: E-mail: [solna@math.utah.edu](mailto:solna@math.utah.edu)

D.W.: E-mail: [washburd@smtpgw1.plk.af.mil](mailto:washburd@smtpgw1.plk.af.mil)

## 2. WAVELET ANALYSIS

Let  $X = (a_0(1), a_0(2), \dots, a_0(2^M))$  denote the data, the temperature recordings. It is convenient to work with data vectors whose length is a power of two because computations are faster for them. In our case  $M$  is between 22 and 23 and we shall work typically with vectors of length  $2^{22} = 4194304$ , corresponding to the first  $84km$  section of the  $112km$  data set. We want to carry out a spectral analysis of  $X$  and to fit the estimated power spectral density to a power law. For this purpose **scale** spectra, rather than Fourier spectra, are a more flexible tool and we will use them here.<sup>4,9</sup>

From the signal we construct successively its wavelet coefficients with respect to the Haar basis as follows. Let

$$a_1(n) = \frac{1}{\sqrt{2}}(a_0(2n) + a_0(2n - 1)) \quad (1)$$

$$d_1(n) = \frac{1}{\sqrt{2}}(a_0(2n) - a_0(2n - 1)) , \quad \text{for } n = 1, 2, \dots, 2^{M-1} \quad (2)$$

be the smoothed signal and its fluctuation, or detail, at the finest scale. Note that the detail vector  $d_1$  contains every other successive difference of the data. This process of averaging and differencing can be continued by defining

$$a_2(n) = \frac{1}{\sqrt{2}}(a_1(2n) + a_1(2n - 1)) \quad (3)$$

$$d_2(n) = \frac{1}{\sqrt{2}}(a_1(2n) - a_1(2n - 1)) , \quad \text{for } n = 1, 2, \dots, 2^{M-2} \quad (4)$$

and in general

$$a_k(n) = \frac{1}{\sqrt{2}}(a_{k-1}(2n) + a_{k-1}(2n - 1)) \quad (5)$$

$$d_k(n) = \frac{1}{\sqrt{2}}(a_{k-1}(2n) - a_{k-1}(2n - 1)) , \quad \text{for } n = 1, 2, \dots, 2^{M-k} \quad (6)$$

for  $k = 1, \dots, M$ . The data vector  $X$  can then be reconstructed from  $a_M, d_M, d_{M-1}, \dots, d_1$  since from equations (1) we have

$$a_0(2n) = \frac{1}{\sqrt{2}}(a_1(n) + d_1(n)) \quad (7)$$

$$a_0(2n - 1) = \frac{1}{\sqrt{2}}(a_1(n) - d_1(n)) , \quad \text{for } n = 1, 2, \dots, 2^{M-1} \quad (8)$$

and now  $a_1$  can be replaced by sums and differences of  $a_2$  and  $d_2$ , etc.

The scale spectrum of  $X$ , relative to the Haar wavelet basis, is the sequence  $S_j$  defined by

$$S_j = \frac{1}{2^{M-j}} \sum_{n=1}^{2^{M-j}} (d_j(n))^2 , \quad j = 1, 2, \dots, M \quad (9)$$

It is easily verified from the definitions above that the  $l^2$  norm of the data vector  $X$  can be written as

$$\sum_{n=1}^{2^M} (a_0(n))^2 = (a_M)^2 + \sum_{j=1}^M 2^{M-j} S_j , \quad (10)$$

which is another way of expressing the orthogonality of the decomposition of  $X$  into  $a_M$  and the  $d_j$ ,  $j = 1, \dots, M$ .

The scale spectral point  $S_j$  is the mean square of the detail coefficients at scale  $j$ . The spectrum can therefore be interpreted as representing the energy of the signal in the different scales.

In Figure 2 we show the first  $20km$  of the temperature data along with  $d_1, d_3, d_5, d_7, d_9, d_{11}, a_{12}$ . The detail coefficients  $d_k$  carry information about the data on larger scales as  $k$  increases. For example,  $d_7$  shows successive

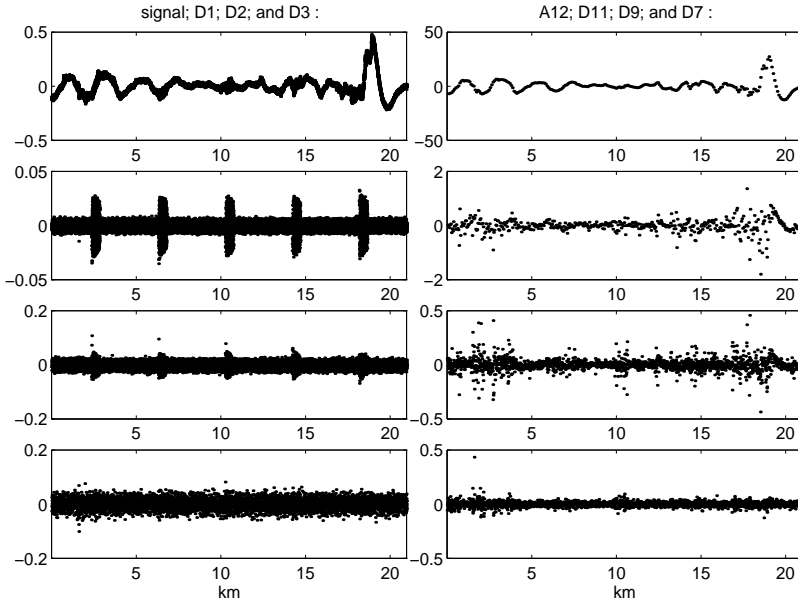


**Figure 2.** Haar wavelet coefficients for the first 21km of the data. The top left figure is the temperature data. The one below it is the  $d_1$  detail coefficients. The third from the top is the  $d_3$  and the bottom the  $d_5$  detail coefficients. Note that the 4km burst seen in  $d_1$  is not visible any more at the  $d_5$  level, after four successive averagings of the data. The top figure on the right is the  $a_{12}$  coefficients and below it  $d_7, d_9, d_{11}$ .

differences of the temperature over distances of  $2.56m$ , after averaging over successive segments of length  $1.28$ . Thus, as  $k$  increases the data are *lowpass* filtered with a filter of decreasing bandwidth and then *subsamped* before the differences are formed. It is clear that the visible periodic components seen in the  $d_1$  coefficients cannot be attributed to turbulence or larger coherent structures in the atmosphere. In the estimation of atmospheric turbulence parameters these spurious features must be suppressed. In  $d_5, \dots$  the high frequency periodic noise component seen above has been effectively suppressed by the lowpass filtering.

### 3. THE SCALE SPECTRUM

Our main objective is now to examine whether the data can be well modeled by a ‘power law’ model over a subrange of scales. A process  $X(x)$  whose structure function has the form

$$E[(X(x_1) - X(x_2))^2] = \sigma^2 |x_1 - x_2|^H . \quad (11)$$

is a *power law* or a *self-similar* process which is not stationary but has stationary increments. For such a process, the scale spectrum  $S_j$  is linear in a log log plot, when the record is very long. In Figure 3 we show log log plots of scale spectra for the temperature data over nonoverlapping segments of the data, with each segment having length  $655m$ . Each plot contains scale spectral points over 15 scales, that is the mean square of  $d_j$ ;  $1 \leq j \leq 15$ . This corresponds to length scales from  $l_1 = .04m$  to  $l_{15} = 655m$ . We take as abscissa the spatial frequency  $K_j$

$$K_j = \frac{1}{l_j} = 50 \cdot 2^{-j} \text{ [rad/m]} . \quad (12)$$

Note that the scale spectra show a distinct departure from power law behavior for scales below one meter ( $K = 1$ ). For larger scales, power law behavior may be considered in the range between  $2.5m$  to  $80m$  ( $.01 \leq K \leq .5$ ), which corresponds to the detail coefficients  $d_7$  to  $d_{12}$ . Of course, the estimated intercept and slope of the log scale spectra depend on the particular segment of data used. We want to identify the part of this variability that is due to the nonstationarity of the process and minimize variability due to estimation errors.

Before we continue with the scale spectral analysis we note the following.

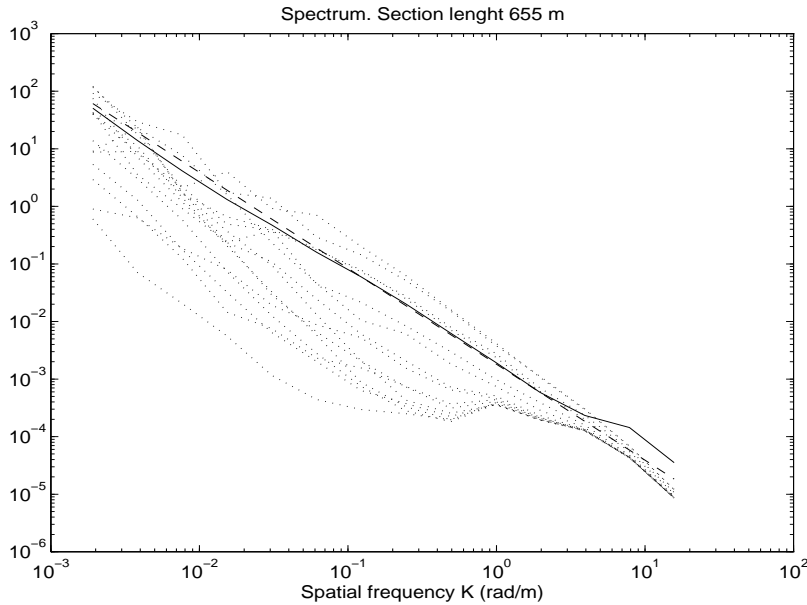


**Figure 3.** Scale spectra of 655m nonoverlapping segments of the data ( $2^{15}$  points per segment) obtained from the Haar wavelet decomposition. The dashed line has slope  $-5/3$  as in Kolmogorov spectra. The solid line is the average over the scale spectra of the different segments. After the averaging is done the scale spectra are plotted in log-log format.

- Noise bursts in the data enter only in some of the detail coefficients, as can be seen from Figure 1. By restricting power law modeling and fitting to scales corresponding to  $d_7, \dots, d_{11}$  the influence of these bursts is effectively eliminated.
- The temperature data are not a stationary time series and they do not have stationary increments. Computing scale spectra over *long* segments, in which the process cannot be taken as stationary, gives a quantity that is hard to interpret. Even though the average slope of the log scale spectra over several segments is close to  $-5/3$ , as the theory of turbulence predicts, there is a lot of variability. A **local** power law model is likely to fit the data better than the idealized power law model, with stationary increments.

We must therefore deal with a larger class of models, local power law processes, and find effective ways to estimate them. We will base our analysis on two criteria. One is that the estimation of parameters should not depend on how the data is segmented. The second is that the variations of the slope and intercept for the log scale spectra must be on length scales that are much longer than those used to compute the spectra themselves. We will show with our analysis that both criteria can be met.

### 3.1. STOCHASTIC MODELING

To illustrate how we cope with non-stationarities consider first the stationary increments case with the process having the structure function (11). Over a suitable range of scales, the mean of the log scale spectrum over a long enough segment is

$$E[\ln(S_j)] \approx c - p \ln(K_j)$$

with  $p = -(2H + 1)$ ,  $c = c(H, \sigma)$  a known function,<sup>10</sup> and  $K_j$  the spatial frequency (12).

Consider a data record of total length  $2^M$  segmented into sections of length  $2^k$ . The (log) spectral points in each segment  $i$  have the form

$$\ln(S_j^i) = c - p \ln(K_j) + w_j^i \quad (13)$$

The spectral point  $\ln(S_j^i)$  is a random variable and  $w_j^i$  is its zero mean random component that depends on both segmentation and scale. By least squares linear fit of the log scale spectra over a suitable range of scales we get estimates of the log-intercept and slope for each segment. These give two processes, one for the slope and one for the log intercept, whose size is  $2^{M-k}$ , the number of segments. Let the slope process  $\{\hat{p}^i\}$  be given by

$$\hat{p}^i = p + v^i \quad (14)$$

with  $v^i$  the random component that *depends on the length of the segment*. Since the estimates are over disjoint sections the  $v^i$  will be almost uncorrelated and we obtain an improved estimate with

$$\hat{p} = \sum_{i=1}^{2^{M-k}} \hat{p}^i / 2^{M-k}. \quad (15)$$

Assume now that we are interested in a *fixed* set of scales and compute the estimate (14) for various segmentation lengths ( $k$ 's). Then the improved estimate (15) and its precision *depend only marginally on the particular segmentation  $k$* . That is, the resulting estimate is not very sensitive to the segmentation of the data.

We now generalize the above to a **local** power law. We model the log scale spectrum by letting

$$\ln(S_j^i) = c^i - p^i \ln(K_j) + w_j^i$$

with  $c^i = c(x_i)$  and  $x_i$  the centerpoint of segment  $i$ . We model  $c$  and  $p$  as *stochastic processes* with spatially varying means but stationary residuals, and with continuous auto-correlation functions. We assume, moreover, that the local power law process itself is conditionally independent of the parameter processes. Our objective is estimation of the parameter processes. We assume that the segmentation length  $2^k$  is short relative to the scale of variation of the parameters. Let  $\hat{p}^i$  denote the estimate of  $p(x_i)$  based on linear regression of  $\ln(S_j^i)$  (with respect to scale), as in (13). To obtain an improved estimate of  $p(x)$ , as in 13, we average or *filter* the process  $\hat{p}(x)$ . The objective here is to minimize the effect of the sampling residual  $w_j^i$ . The filter will depend on the stochastic structure of  $p(x)$ . The improved estimate can now be expressed as

$$\tilde{p}^i = \sum_{l=1}^{2^{M-k}} \lambda^i(l) \hat{p}^l. \quad (16)$$

with  $\lambda^i(l)$  the filter coefficients. *After* filtering, the estimates of the slope and log intercept are much less sensitive to the segmentation, since these are chosen to be short relative to the scale of variation of the parameters. The filter in (16) is given explicitly below.

### 3.2. SEGMENTATION DEPENDENT ESTIMATION

We begin by selecting four segmentations and estimating slopes and intercepts for the scale spectra obtained for each segment, as shown in Figure 4. The four segmentations are:

$$160m \ (2^{13} \text{ points}), \ 327m \ (2^{14}), \ 655m, \ (2^{15}), \ 1.31km \ (2^{16}).$$

There are 512, 256, 128, 64 nonoverlapping segments, respectively, in each case. Within each segment we use only scale spectra from  $d_7$  to  $d_{11}$ , corresponding to length scales between  $2.5m$  and  $80m$ . We limit the longer scales to  $40m$ , well below the shortest segmentation length which is  $160m$ . We limit the shorter scales to  $2.5m$  because, as can be seen from Figure 3, below that scale the spectrum changes and power law fit is not appropriate. The fitting is done by a generalized least squares linear regression model

$$\log S_j^i \approx c^i - p^i \log\left(\frac{2^j}{50}\right), \quad j = 7, 8, \dots, 11$$

for each segment  $i$ , and the units are adjusted so that the horizontal axis is in kilometers.

We see from Figure 4 that the estimated slopes,  $p$ , and the log intercepts,  $c$ , vary considerably over the 80 kilometer data set. They also depend on the segmentation, with the finer one having larger fluctuations (dotted lines). We next carry out the filtering, as indicated above, in order to remove the sampling variability that is segmentation dependent.

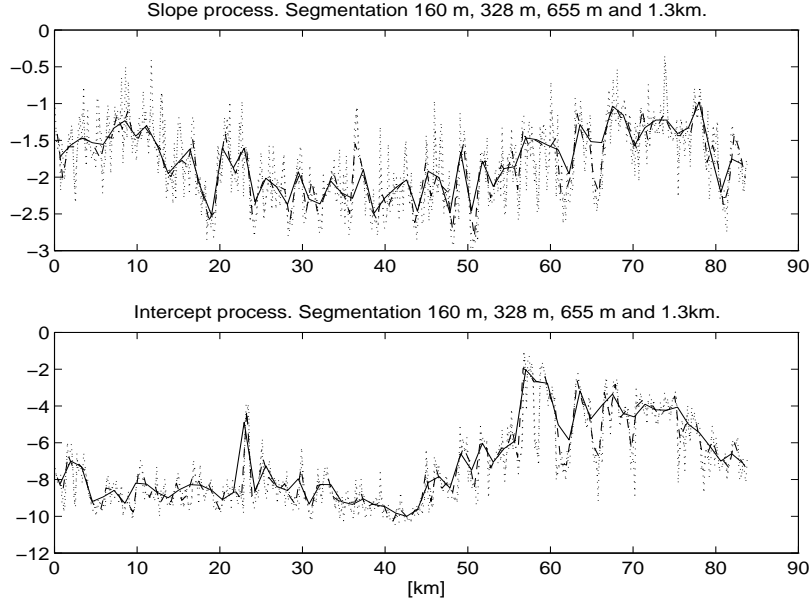


**Figure 4.** Top figure: slopes of log-log scale spectra from wavelet decompositions based on four different segment lengths. At the finest resolution the scale spectra are calculated over nonoverlapping segments 160m long. This is the dotted line that has the largest variations. At the next resolution the nonoverlapping segments are 327m long (also plotted with a dotted line). The other two resolutions are 655m and 1.31km and are shown with dashed and solid lines, respectively. The bottom figure is the same as the top but now for the log intercept of the scale spectra.

### 3.3. REMOVAL OF SEGMENTATION EFFECTS

Our objective is to remove, to the extent possible, the effects of the segmentation dependent sampling variability in the parameter estimates. Recall that the parameters are modeled as

$$\hat{p}^i = p^i + v^i,$$

for the slope, with  $v^i$  the noise to be filtered out. We shall construct the filter to give the minimum variance unbiased estimates for the parameter processes  $p^i$  and  $v^i$ . For this we need the parameters in the stochastic models for these processes. We assume that the slope process is exponentially correlated. We need, therefore, its correlation length  $l_p$  and its variance  $\sigma_p^2$ , in addition to the location dependent mean ( $\bar{p}_i$ ). Then

$$\begin{aligned} E[p_i] &= \bar{p}_i \\ E[(p_i - \bar{p}_i)(p_j - \bar{p}_j)] &= \sigma_p^2 \exp(-L|i - j|/l_p) \end{aligned} \quad (17)$$

with  $L$  the length of the segments. Note that this model is intrinsic to the process and does not depend on the segmentation. As discussed above we shall model the sample noise process  $\{v_i\}$  as white, so we only need its level  $\sigma_v^2$ .

Before estimating these model parameters we discuss the filter that is defined in terms of them. Let  $\hat{\mathbf{P}} = (\hat{p}_i)$  be the vector of estimates,  $\mathbf{P} = (p_i)$  the realization of the slope process and  $\bar{\mathbf{P}} = (\bar{p}_i)$  the mean. Then the filter  $\Gamma$  is a matrix that transforms  $\hat{\mathbf{P}}$  into  $\Gamma\hat{\mathbf{P}}$  in such a way that

$$E[||\Gamma\hat{\mathbf{P}} - \mathbf{P}||^2]$$

is minimized over all matrices  $\Gamma$  that also preserve the mean  $\bar{\mathbf{P}}$  of  $\mathbf{P}$ , that is  $\Gamma\bar{\mathbf{P}} = \bar{\mathbf{P}}$ . Let  $C_p$  be the covariance matrix of  $\mathbf{P}$  (determined by  $\sigma_p$  &  $l_p$ ), then it easily follows that

$$\Lambda = (C_p + \sigma_v^2 I)^{-1} [C_p + \mathbf{u}^T \otimes \bar{\mathbf{P}}]$$

where the vector  $\mathbf{u} = (u_i)$  is given by

$$u_i = \frac{\bar{\mathbf{P}}_i - \bar{\mathbf{P}}'(C_p + \sigma_v^2 I)^{-1} C_{p,i}}{\bar{\mathbf{P}}'(C_p + \sigma_v^2 I)^{-1} \bar{\mathbf{P}}}.$$

Here  $C_{p,i}$  is the  $i$ -th column of the matrix  $C_p$  and the superscript  $T$  stands for transpose. The slope and log intercept processes are filtered separately. Filtering of this kind is discussed in.<sup>7</sup>

Having defined the filter we next discuss estimation of the model parameters involved in its definition. We can extract from the slope and log intercept process of Figure 4 the smooth, background variations. This defines our estimate of  $\bar{\mathbf{P}}$  in the case of the slope process as well as the log intercept process. It can be done with a simple moving average but we used a three term matching pursuit<sup>5</sup> procedure.

We estimate the parameters  $\sigma_p^2$ ,  $l_p$  and  $\sigma_v^2$  using the empirical variogram. For a time series  $\mathbf{X} = (X_i)$  of size  $N$  the empirical variogram with lag  $j$  is defined by

$$V(j) = \frac{1}{2(N-j)} \sum_{k=1}^{N-j} (X_{k+j} - X_k)^2 \quad (18)$$

with dependence on the length of the data vector  $N$  not shown. Observe that since the mean of  $\mathbf{P}$  varies slowly relative to the sampling interval, the empirical variogram is essentially unaffected by variations in the mean. The mean of the empirical variogram for the slope process  $\hat{\mathbf{P}}$  is

$$E[V(j)] = \sigma_p^2 \exp(-L|i-j|/l_p) + \sigma_v^2$$

and from this follow the parameter estimates by fitting to the empirical variogram. In particular,  $\sigma_v^2$  is given by the vertical intercept since, according to our assumptions, the process  $\{v_i\}$  is white. This will be verified by the simulations in the next section and is supported by our analysis in.<sup>10</sup> The estimated parameters are as follows:

- **For the slope:** Vertical intercept  $\sigma_n^2 = 0.09$ , horizontal asymptote level  $\sigma_n^2 + \sigma_s^2 = 0.21$ , and correlation length  $640m$  (four segment lengths).
- **For the log intercept:** Vertical intercept  $\sigma_n^2 = 0.13$ , horizontal asymptote level  $\sigma_n^2 + \sigma_s^2 = 1.83$ , and correlation length  $480m$  (three segment lengths).

The variogram was also computed for the other segmentations and gave consistent values. However, for the coarsest segmentation the assumption that the correlation length is much larger than the segment length is violated and the parameter estimates become less precise.

Based on the estimated model parameters we can carry out the filtering to get a better estimate for the slope and log intercept processes. In Figure 5 we show these filtered slope and intercept processes. Note that after the filtering all four segmentations give essentially the same result. This is a very strong indication that the model we have chosen and the analysis that we have followed fit the aerothermal data very well. Recall, however, that the correlation length of the slope and log intercept processes were approximately  $500m$ . Therefore, when the spectrum parameters are estimated based on the two coarsest segmentations ( $655m$  and  $1.3km$ ), they are smoothed somewhat and the estimates do not represent their variability faithfully. This is verified by Figure 5, since the two dotted curves, corresponding to the coarser resolutions, are somewhat smoothed versions of the solid line that corresponds to the two finest resolutions.

## 4. SIMULATION AND MODEL VALIDATION

### 4.1. CONDITIONAL SIMULATION

We next simulate synthetic temperature profiles using the parameters estimated above. Our objective is to examine the modeling assumptions used above and also the accuracy of the estimates. The simulations will be *conditioned* on the slope and log intercept processes of Figure 5. In the next subsection we contrast these simulations with those based on simulating from the full model, that is with slope and log intercept processes drawn from the model (17).

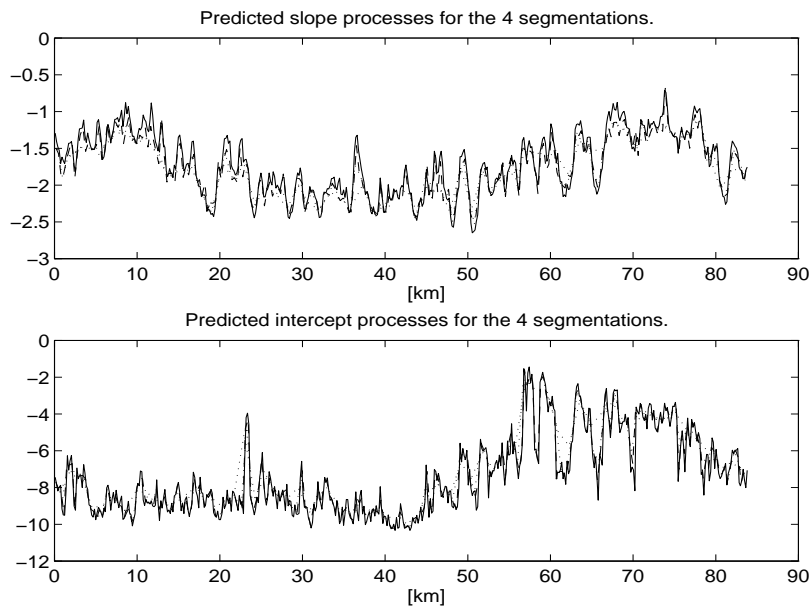


**Figure 5.** Filtered slope (top) and log intercept (bottom) processes of the actual data for the four different segmentations. Note that all four segmentations of the filtered processes are essentially the same. The solid and dashed lines correspond now to the two finest resolutions and are indistinguishable. The dotted curves correspond to the two coarsest segmentations and are slightly smoother versions of the other curves. The filtering has eliminated the differences in the slope and log intercept processes that are due to the segmentation (as in Figure 4) by removing the white noise component of the slope and log intercept fluctuations that is due to sampling.

The realizations that we generate are Gaussian, local power law processes. The realizations have common features with the data shown in Figure 1. However, the noise in the measurements makes a direct comparison difficult. Recall that we only aim at modeling the data on a subset of scales, the scales corresponding to  $d_7 - d_{11}$ . A better way to compare the processes is when both have been *scale* filtered so that only scales  $d_7 - d_{11}$  contribute. This correspond to length scales in the range  $2.5 - 80m$ , which are the ones we used in estimating slopes and log-intercepts of the power law. Figure 6 shows the results. The similarity between the processes is striking.

The slopes and log-intercepts processes of Figure 4 are obtained by fitting the log scale spectra from  $d_7 - d_{11}$ , in each segment. We measure the error in the fit by the sum of squares of the differences of the log spectra from the fitted line. This quantity provides another way to test our modeling. The discrepancy in each section defines a random process. If indeed the measured data can be regarded as a realization from the model this discrepancy should be similar for measured and synthetic data. In Figure 7 we plot the discrepancy corresponding to the measurements and also a realization, both normalized by the mean of the discrepancy of the latter. They are similar, supporting the conclusion that over the targeted set of scales the temperature data is modeled well by the local power law process.

Consider the model for the temperatures defined by letting the slopes and log-intercepts be the smooth ‘background’ processes. Is this a better model for the temperatures? We examine this by calculating the same quantity as in the previous Figure, the discrepancy between the data and a realization from this alternative model. The result indicates that this is not a better model since the discrepancies are now very different.

Consider now the simulated data. We can analyze them in the same way as the measured data and get estimates of the slope and log intercepts of their scale spectra. We present the correlation structure of the parameter processes estimated in this way in Figure 8. The correlations are calculated using the empirical variogram. The stars in the plot corresponds to calculating the variogram of the difference between the estimated parameters and the specified ones. This corresponds to what we referred to above as sampling error. As expected the sampling error is essentially a white noise process. The crosses in the Figure are the variogram of the slope process relative to the smooth background. The solid line is the fitted model. There are two parts to it, the sampling noise part (the intercept) and



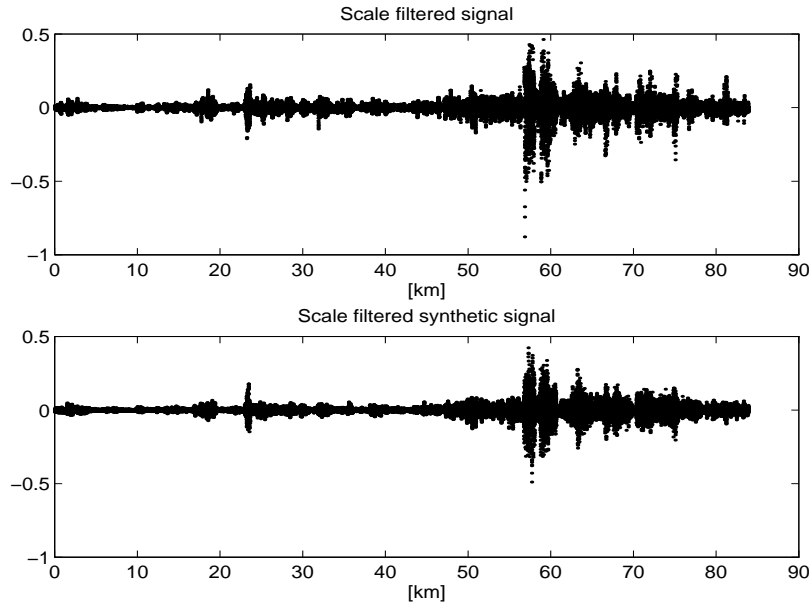


**Figure 6.** The *actual* temperature data set (top figure) obtained by synthesizing it from the detail coefficients  $d_7 - d_{11}$  of its Haar decomposition. It is information from this range of scales that enters into the slope and intercept processes. The bottom figure is the same as the top but for the *simulated* data. Note the striking similarity between the two figures.

the exponential part corresponding to intrinsic variation in the parameters. The intercept part is seen to match well with that obtained for the sampling noise of the synthetic data. The match for the exponential part is not so good. This is because the filtering that suppresses the sampling noise also smooths out some of the intrinsic variation in the parameters. This is seen from the circle plot in Figure 8 showing the variogram for the specified parameters. The fit is now much better.

Let us also comment on the accuracy of the parameter estimates. We do this by simulation. The standard deviation between the specified and estimated parameters for the slope and log-intercept estimates are .08 and .2, respectively.

#### 4.2. REPLICATION FROM THE FULL MODEL

We now simulate the temperature data from the full model, that is with the slope and log intercepts sampled from from 17 with the estimated model parameters. Two realization are shown in Figure 9, middle and bottom part. The parameters of the realization shown on the top plot, corresponding to a conditional simulation, are overly smoothed because of the filtering. The realization of this section will therefore have more variability. This is seen in Figure 10. Clearly the differences for the full simulation (bottom) plot are more variable than those for a realization conditioned on the filtered parameter sequences (top plot).

### 5. SUMMARY AND CONCLUSIONS

The main premise driving our analysis of temperature data from a turbulent atmosphere is that it is a local power law process. This means that the power law itself (the exponent (slope) and the multiplicative constant (log intercept)) are not constants but slowly varying functions. We estimate the slope and log intercept of the scale spectrum by appropriately segmenting the data and then removing segmentation effects by a filtering process. The slope and log intercepts themselves are modeled as stochastic processes. We generate synthetic temperature in two different ways. First, the local power law process is simulated conditioned on the particular parameters estimated from the data (slope and log intercept). Then we get a faithful replication of the temperature data. Second, the parameters are taken as random, that is sampled from their model. Then the simulation is sample-wise very different from the

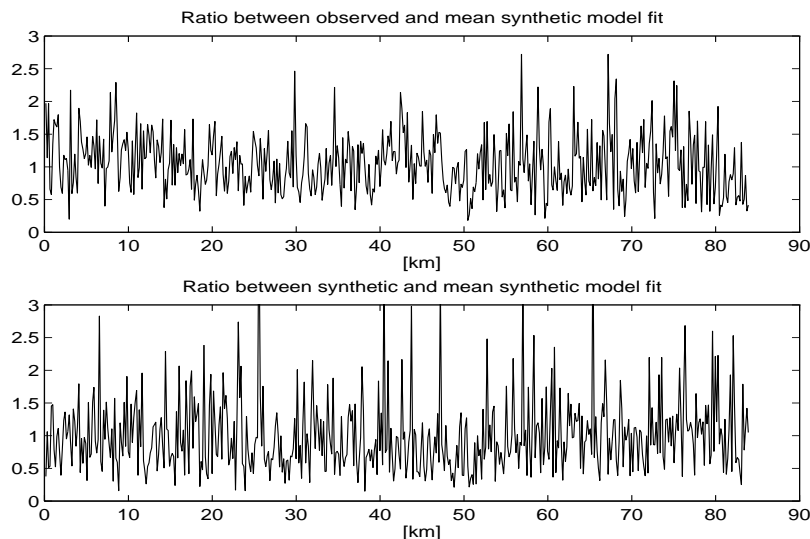


**Figure 7.** Top: The ratio of the  $l^2$  norm of the difference between the log-log scale spectrum and the power-law fitted log-log spectrum for the *actual* data (finest segmentation,  $2^{13}$  points each) over the mean (over the 512 segments) of the  $l^2$  norm of the difference between the scale spectrum and the power-law fitted spectrum for the *simulated* data. Bottom: Same as for the top figure with only simulated data. The scale spectrum corresponding to  $d_7$  to  $d_{11}$  is used in calculating the  $l^2$  error and in the power law fit. This contains information in the data over length scales of  $2.5m$  to  $80m$ .

actual data, but the statistics are faithfully reproduced. This and the removal of segmentation effects is a very strong indication that the model and the analysis that we have followed capture the essential features of the data.

An important aspect of the model that we use is separation of scales in the variation of the estimated parameters (slope and log intercept) from the underlying process that generates the power law spectra. The wavelet transform plays, moreover, a central role in our analysis.

## 6. ACKNOWLEDGEMENT

This work was done in close collaboration with C. Rino and V. Kruger of Vista Research in Mountain View California. A detailed account is in.<sup>11</sup>

## REFERENCES

1. D. C. Washburn, D. W. banton, T. T. Brennan, W. P. Brown, R. R. Butts, S. C. Coy, R. H. Dueck, K. W. Koenig, B. S. Masson, P. H. Peterson, R. W. Praus, G. A. Tyler, B. P. Venet and L. D. Weaver, Airborne laser extended atmospheric characterization experiment (ABLE ACE). Technical report, Phillips Laboratory, Kirtland Air Force Base NM 87117-5776, May 1996.
2. M. Kim and A. H. Tewfik, Multiscale signal detection in fractional Brownian motions, SPIE, 1348, pp. 462-470, 1990.
3. P. Flandrin, Wavelet Analysis and Synthesis of Fractional Brownian Motion, IEEE Trans. Information Theory, 38, pp. 910-917, 1992.
4. P. Abry, P. Goncalves and P. Flandrin, Wavelets, spectrum analysis and  $1/f$  processes, in 'Wavelets and Statistics', A. Antoniadis and G. Oppenheim editors, Springer Lecture Notes in Statistics 103, Springer 1995.
5. S. Mallat and Z. Zhang, Matching pursuit in a time-frequency dictionary, IEEE Trans. Signal Processing, 41, pp. 3397-3415, 1993.
6. H. Omre, K. Solna and H. Tjelmeland, Simulations of random functions on large lattices, in 'Geostatistics', A. Soares editor, pp. 179-199, Kluwer Academic Publishers, 1993.

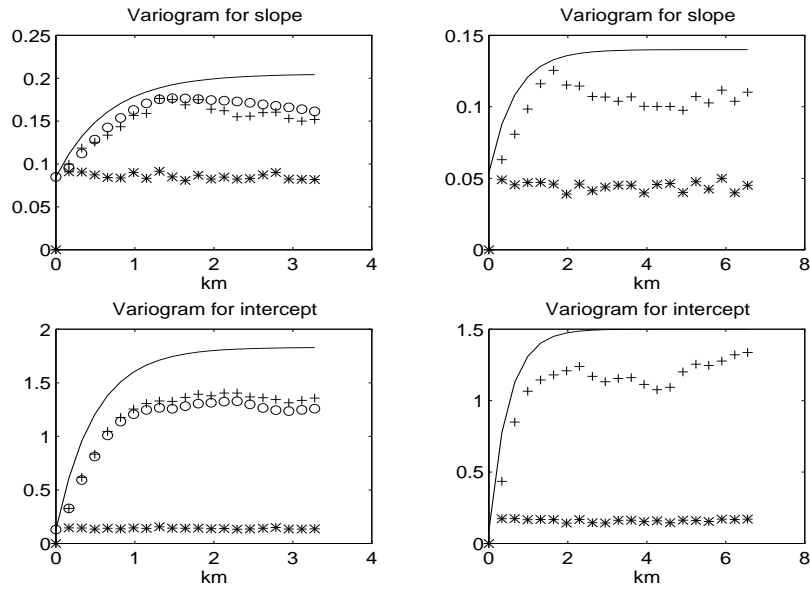


**Figure 8.** Variograms for the fluctuations of the slope (top) and log intercept (bottom) processes obtained from the simulated temperature data. The stars are computed from the fluctuations when the filtered background is subtracted. The solid curves are exactly the ones fitted to the *actual* data. The circles are the variogram of the specified parameters obtained from the data. The crosses are variograms for fluctuations when only the smooth background is subtracted. The curves on the left are from data at the finest, 160m, resolution while those on the right are for the next to finest, 330m.

7. B. Ripley, *Spatial Statistics*, Wiley, New York, 1981.
8. I. Karatzas and S. E. Shreve, *Brownian Motion and Stochastic Calculus*, Springer-Verlag, New York, 1991.
9. G. Kaiser, *A Friendly Guide to Wavelets*, Birkhäuser, 1994.
10. G. Papanicolaou and K. Solna, *Estimation of a locally turbulent process*, preprint, 1998.
11. V. Kruger, C. Rino, G. Papanicolaou and K. Solna, *Analysis of Aerothermal Data*, Vista Research Report, Mt. View CA, February 1998.

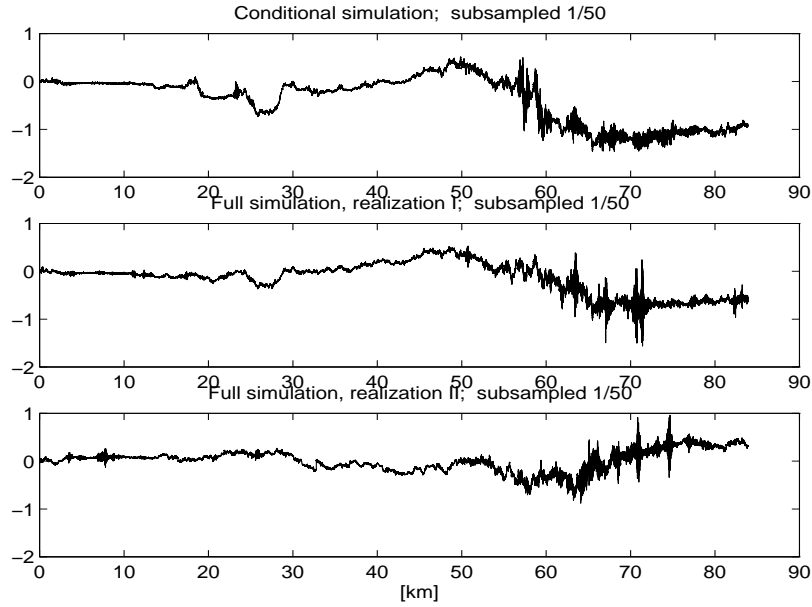


**Figure 9.** Two different realizations of simulated temperature data (top and bottom figures) in which the slope and log intercept are Gaussian stochastic processes with the estimated model parameters. The slope and the log intercept fluctuations are generated from the same white noise sequence that is independent of the power law process.

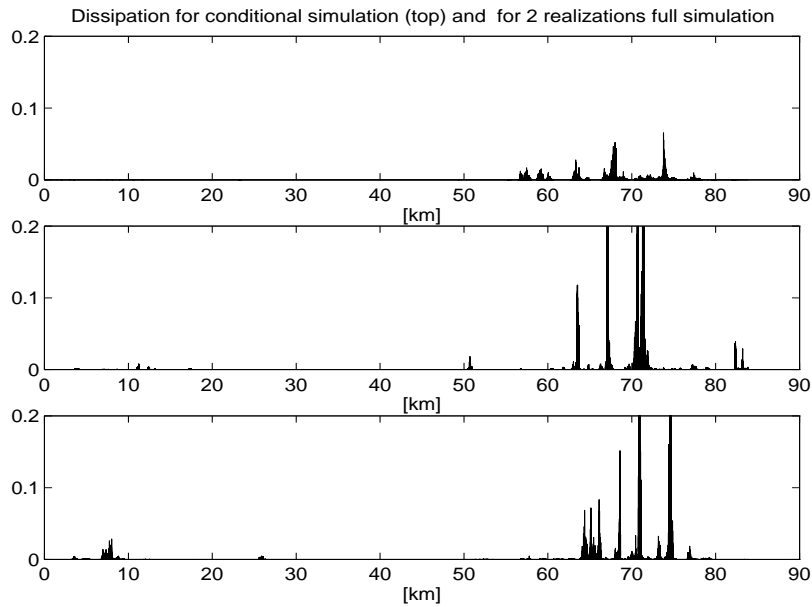


**Figure 10.** Absolute values of temperature differences for the conditional simulation with deterministic slope and intercept (top figure) and for the top of Figure 9 (bottom figure).